

A Compact UWB Antenna Design Using Rounded Inverted L-Shaped Slots and Beveled Asymmetrical Patch

Aliakbar Dastranj* and Faezeh Bahmanzadeh

Abstract—A compact ultra-wideband (UWB) antenna with simple structure is presented. To achieve UWB performance with a compact size, two open ended rounded inverted L-shaped slots are etched on the square ground plane. Moreover, further bandwidth enhancement is obtained by cutting a bevel on the asymmetrical radiating patch. The antenna is fed by a $50\ \Omega$ microstrip line and has a small size of $28 \times 28 \times 1.6\ \text{mm}^3$. The simulation time- and frequency-domain results obtained from HFSS simulator package are verified by experimental measurements. Both simulated and measured results show that the antenna can provide a wide impedance bandwidth of more than 129% from 2.7 to 12.55 GHz with -10 -dB reflection coefficient. Besides, it is shown that by introducing several antenna designs, the impedance bandwidth can be enhanced from 58% to 129%. The effects of the key design parameters on the antenna impedance bandwidth are also investigated and discussed. Measured results for the reflection coefficient, far-field radiation patterns, radiation efficiency, gain, and group delay of the designed antenna over the UWB spectrum are presented and discussed. Measured data show good concordance with the numerical results. Also, the fidelity factor is calculated in both E - and H -plane by using CST Microwave Studio. The obtained results in both time- and frequency-domain indicate that the antenna is a good option for UWB applications.

1. INTRODUCTION

Over the past decade ultra-wideband (UWB) technology has attracted much attention of large number of researchers. UWB wireless communication system covers a very wide spectrum of frequencies that ranges from 3.1 to 10.6 GHz [1]. As antennas are key components of any UWB wireless system, it is essential that they have UWB performance particularly with respect to impedance and radiation characteristics. Also, in these systems, high-performance antennas are required to have the characteristic of low-profile [2–4]. Compared with the traditional wide band antennas such as Vivaldi, log-periodic and spirals, slot antenna becomes an attractive candidate to realize a broadband and UWB characteristics due to its low profile, wide bandwidth, compact size, low cost, and ease of fabrication as well as easy integration in active components and monolithic microwave integrated circuits [5–8].

In the last few years, to improve the impedance bandwidth of planar slot antennas, several techniques have been proposed. One method is to use different geometries of slots [9–16], and the other techniques use several tuning stubs to achieve wideband performance [17, 18]. Among different slot geometries, those worthwhile mentioning are binomial-curve [9], annular-ring [10], fractal [11], rhombus [12], elliptical and circular [13], rectangle [14], triangle [15], and square [16]. The impedance bandwidths of these antennas are less than 104%. In [17], by using a coplanar waveguide (CPW) feed with a widened tuning stub, a square slot antenna with dimensions of $72\ \text{mm} \times 72\ \text{mm}$ can yield a bandwidth of 60%. The design of a UWB CPW-fed slot antenna etched on a 0.813-mm-thick substrate with a U-shaped tuning stub for bandwidth enhancement is presented in [18]. It features an impedance bandwidth

Received 17 November 2017, Accepted 7 December 2017, Scheduled 16 January 2018

* Corresponding author: Aliakbar Dastranj (dastranj@yu.ac.ir).

The authors are with the Department of Electrical Engineering, Faculty of Engineering, Yasouj University, Yasouj, Iran.

of 110% and bidirectional radiation patterns with an average gain of about 2 dBi. A round corner rectangular wide-slot antenna with a size of $68 \times 50 \text{ mm}^2$ is proposed in [19]. The impedance bandwidth of the antenna with -10 -dB reflection coefficient is almost two octaves from 2.08 to 8.25 GHz. In [20], a printed slot antenna loaded with small heptagonal slots is investigated. The small perturbations are added in the corners of the main slot antenna to provide a multi-resonance operation. As a result, a wide impedance bandwidth of 105.3% is achieved. Two printed slot antennas with equal sizes of $110 \text{ mm} \times 110 \text{ mm}$ and impedance bandwidths of 120% (1.82 to 7.23 GHz) and 110% (2.42 to 8.48 GHz) are presented in [21]. In [22], based on a rotated square slot resonator a printed slot antenna with a parasitic patch for bandwidth enhancement is proposed. By properly choosing the suitable slot shape, embedding the similar parasitic patch shape, and tuning their dimensions, a wide operating bandwidth ranging from 2.225 to 5.355 GHz is obtained. An open-slot antenna with a wide impedance bandwidth of 122% is designed in [23]. Two bevels are cut on the patch to enhance the impedance bandwidth. A compact CPW-fed antenna with a half-elliptical-edged monopole radiator and two symmetrical open-circuit stubs extended from the ground plane is proposed in [24]. Its impedance bandwidth ranges from 3.7 to 10.1 GHz. Two UWB CPW-fed printed antennas with dimensions of $50 \times 50 \text{ mm}^2$ and $48 \times 42 \text{ mm}^2$ and impedance bandwidths of 118.8% and 125% are reported in [25] and [26], respectively. Recently, a bandwidth-enhancement method of using a new radiator with a hybrid square-circular configuration and a rectangular open slotted ground plane with a pair of symmetrical I-shaped tuning stubs was introduced to implement a CPW-fed planar monolayer UWB antenna with a size of $44 \times 32 \times 1.6 \text{ mm}^3$ [27].

In this paper, a low-profile asymmetrical microstrip-fed UWB antenna with a simple structure is designed and successfully implemented. The novelty of the proposed design lies in its simple configuration and simplicity to obtain the desired antenna characteristics in both time- and frequency-domain. Multiple resonances and consequently UWB performance with a compact size are achieved by etching two open ended rounded inverted L-shaped slots on the square ground plane. Also, further bandwidth enhancement is obtained by cutting a bevel on the asymmetrical radiating patch. The simulation time- and frequency-domain results obtained from HFSS simulator package are verified by experimental measurements. Measured results show that the proposed antenna has a wide impedance bandwidth of more than 129% from 2.7 to 12.55 GHz (for $|S_{11}| < -10 \text{ dB}$) which can cover the whole UWB spectrum (3.1–10.6 GHz). In addition, the antenna has a simple structure with a small size of $28 \times 28 \times 1.6 \text{ mm}^3$. Compared with the recent designs presented in [25] and [26], the designed antenna has a smaller size and wider bandwidth. This comparison reveals the advantages of the proposed antenna. The development stages of the proposed antenna are presented, and several designs are investigated. It is shown that by introducing several antenna designs, the impedance bandwidth can be enhanced from 58% to 129%. The effects of the key design parameters on the antenna impedance bandwidth are also investigated and discussed. Measured results for the reflection coefficient, far-field radiation patterns, radiation efficiency, gain, and group delay of the designed antenna over the entire frequency band of interest are presented and compared with the simulation outcomes. The simulated and measured results show good agreement over the entire ultra-wide bandwidth. Also, the fidelity factor is calculated in both E - and H -planes by using CST Microwave Studio. Based on the measured results, the proposed antenna is very suitable for several UWB applications.

2. ANTENNA DESIGN AND DEVELOPMENT STAGES

Figure 1 shows the geometry and design parameters of the proposed antenna. As shown in this figure, the proposed structure has a truncated rectangular radiator which is fed asymmetrically by a 50Ω microstrip line. In order to accomplish UWB performance of the antenna two open ended inverted L-shaped slots are etched on the square ground plane and the corners of the open ended L-shaped slots are rounded. Moreover, to improve the impedance matching of the antenna, a small inverted L-shaped slot is etched on the ground plane in the bottom side of the antenna. The designed antenna with the total area of $28 \times 28 \text{ mm}^2$ was printed on an FR4 substrate with a relative permittivity of $\epsilon_r = 4.4$, thickness of 0.8 mm, and loss tangent of 0.02. The geometrical parameters of the radiator and ground plane are as follows: $Lg = 26 \text{ mm}$, $Wg = 20 \text{ mm}$, $Wf = 1.53 \text{ mm}$, $Lp = 6 \text{ mm}$, $Wp = 9 \text{ mm}$, $Ls = 6 \text{ mm}$, $Ws = 2.7 \text{ mm}$, $S = 0.7 \text{ mm}$, $L1 = 14 \text{ mm}$, $L2 = 2.75$, $L3 = 6 \text{ mm}$, $L4 = 2 \text{ mm}$, $W1 = 2 \text{ mm}$, $W2 = 2.75 \text{ mm}$, $W3 = 8.235 \text{ mm}$, $R = 3 \text{ mm}$, and $G = 0.55 \text{ mm}$. The numerical analysis and geometry

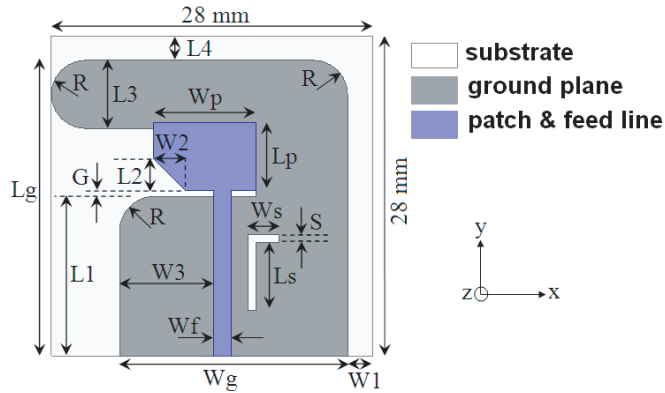


Figure 1. Geometry and design parameters of the proposed antenna.

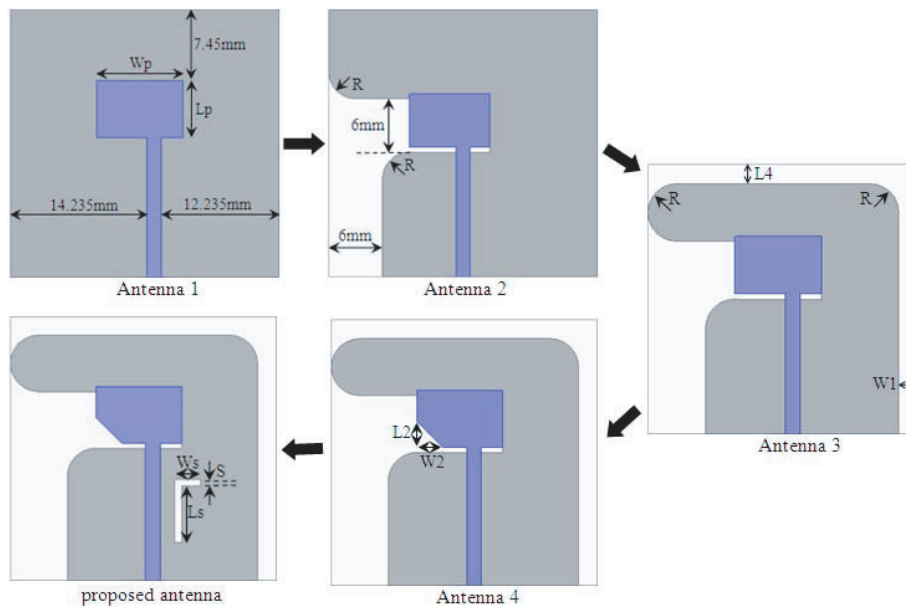


Figure 2. Stages of the antenna design.

refinement of the proposed antenna are performed by using Ansoft HFSS, a full-wave electromagnetic simulator package which is based on the finite element method. As will be shown in the following, by using the aforementioned techniques, multiple resonances and consequently a broad bandwidth of 129% (2.7 to 12.55 GHz for $|S_{11}| < -10$ dB) can be obtained.

The development stages of the proposed antenna are illustrated in Figure 2, and the corresponding simulated reflection coefficient curves are plotted in Figure 3. The design procedure begins with the design of Antenna 1. As shown in Figure 2, Antenna 1 consists of square ground plane (28×28 mm²) and a rectangular radiator which is asymmetrically fed by a 50Ω microstrip line. Referring to Figure 3, it can be observed that Antenna 1 provides a -10 -dB reflection coefficient bandwidth of about 4.5% from 7.6 to 7.95 GHz. After etching the first open ended inverted L-shaped slot on the square ground plane and rounding the corners of the slot (Antenna 2), multiple resonances are generated and the antenna can get multiband operation with -10 -dB impedance bandwidths of about 19% (2.8–3.4 GHz), 58% (4.6–8.4 GHz), 9.8% (9.7–10.7 GHz), and 9.1% (11.5–12.6 GHz), respectively. In the next step, the second open ended inverted L-shaped slot is etched on the ground plane (Antenna 3), and as depicted in Figure 3, dual-band operation with two impedance bandwidths of 120% (2.7–10.8 GHz) and 4.8% (12.1–12.7 GHz) is resulted. In this case, Antenna 3 satisfies the requirement for UWB systems.

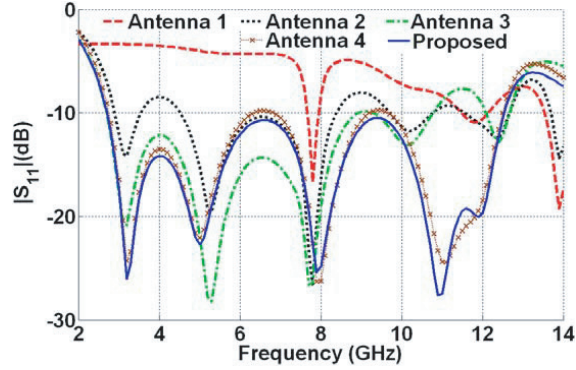


Figure 3. Simulated reflection coefficient curves of the antennas corresponding to Figure 2.

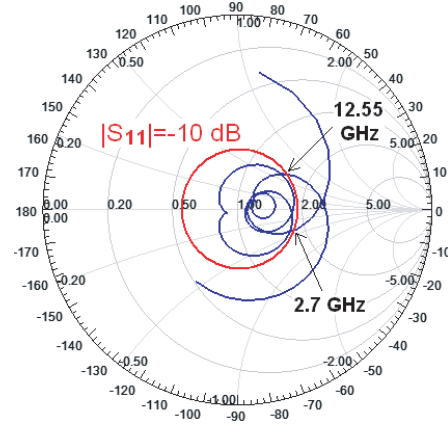


Figure 4. Simulated input impedance on Smith chart of the proposed antenna.

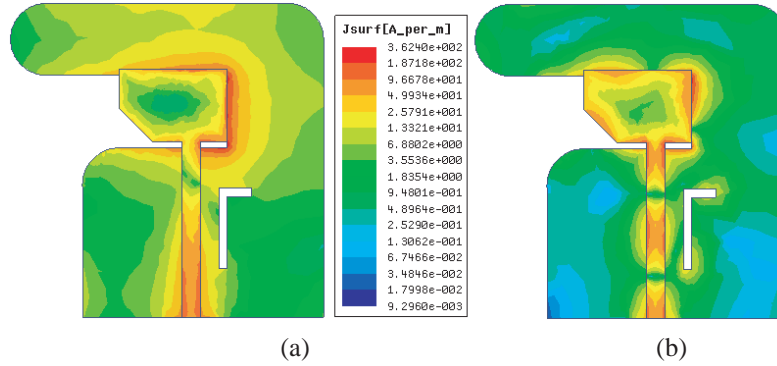


Figure 5. Simulated surface current distributions on the proposed antenna. (a) At 3 GHz. (b) At 12 GHz.

Afterwards, to enhance the impedance bandwidth of the antenna, one corner of the radiator is truncated (Antenna 4) and as shown in Figure 3, the fourth resonant frequency is occurred at about 11 GHz. As a result, Antenna 4 can cover the broad frequency range of 2.7–12.55 GHz. However, in the last step of the antenna design, to improve the impedance matching of the antenna at the middle frequencies (6.5 and 9.5 GHz), a small inverted L-shaped slot is etched on the ground plane (proposed antenna). As illustrated in Figure 3, the proposed antenna features good impedance matching over the entire frequency range of 2.7–12.55 GHz. Its impedance bandwidth is more than 129% for $|S_{11}| < -10$ dB. The evolution procedure discussed above clearly shows that the two open ended inverted L-shaped slots corner truncated radiator, and small inverted L-shaped slot collaboratively establish the UWB performance of the antenna.

In order to further investigate the impedance characteristic of the proposed antenna, the simulated input impedance on Smith chart of the proposed antenna is plotted in Figure 4. This figure shows four loops on the Smith chart, which are related to four resonant frequencies illustrated on the reflection coefficient plot of Figure 3. Moreover, it can be observed that these loops are completely inside the $|S_{11}| = -10$ dB circle, and the proposed antenna has a simulated -10 -dB impedance bandwidth ranging from 2.7 to 12.55 GHz.

The surface current distribution on the antenna radiator and ground plane at 3 and 12 GHz is presented in Figure 5. It is seen that the current distribution at the lower frequency, 3 GHz, is considerably concentrated on the ground plane, while at the higher frequency, 12 GHz, current distribution is mainly concentrated on the truncated radiator. This means the ground plane and radiator affect the impedance characteristic at low and high frequencies, respectively.

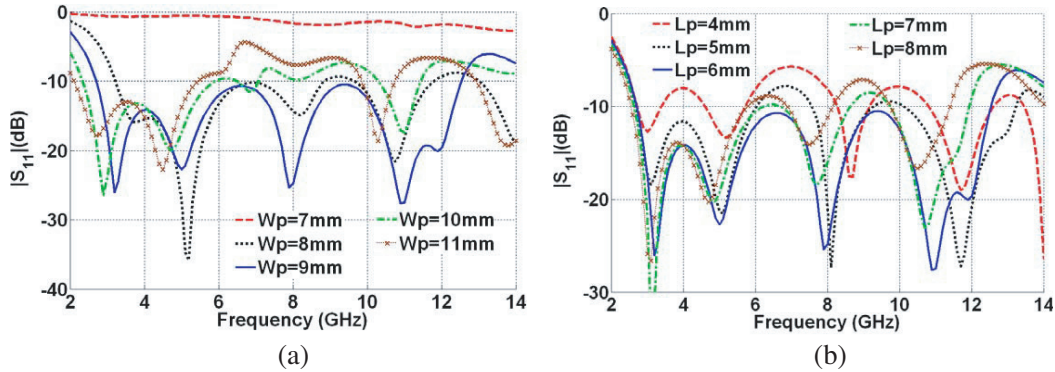


Figure 6. Influence of W_p and L_p on the impedance bandwidth of the antenna. (a) W_p . (b) L_p .

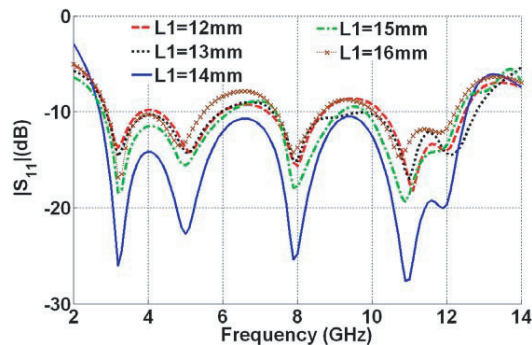


Figure 7. Influence of L_1 on the impedance bandwidth of the antenna.

Numerical parametric analysis via Ansoft HFSS was performed to understand the influence of the antenna physical dimensions on the impedance bandwidth. Figure 6 shows the influence of the rectangular radiator dimensions, W_p and L_p , on the antenna impedance characteristic. It is seen that these geometrical parameters affect the impedance matching of the antenna over the whole band of interest. It should be noted that L_p does not affect the lower band edge frequency of the antenna (see Figure 6(b)). Figure 6 shows that selecting the optimal values of $W_p = 9$ mm and $L_p = 6$ mm leads to widest bandwidth. The influence of L_1 on the antenna impedance bandwidth is illustrated in Figure 7. As depicted in this figure, by increasing L_1 from 12 to 14 mm, the antenna reflection coefficient improves in 2.7–12.55 GHz frequency range. However, by further increasing L_1 to 16 mm, the antenna reflection coefficient increases spatially at the frequencies about 7 and 9 GHz. Results of Figure 7 show that the optimum value of this parameter for maximum impedance bandwidth is 14 mm.

3. NUMERICAL AND EXPERIMENTAL RESULTS

In order to validate the numerical results obtained by Ansoft HFSS, the proposed antenna was constructed and tested inside a microwave anechoic chamber. Figure 8 shows the fabricated prototypes of the antennas. In the following, the experimental outcomes in frequency- and time-domain are given, discussed, and compared with the numerical results.

Figure 9 presents the comparison of experimental and numerical reflection coefficients of the antenna. The experimental result shows excellent agreement with the simulated one, which validates the design procedure. Both measured and simulated results indicate that the proposed antenna features desirable impedance matching over a wide spectrum, from 2.7 to 12.55 GHz (129% impedance bandwidth for $|S_{11}| < -10$ dB). However, to determine the overall bandwidth of the antenna, other radiation parameters of the antenna such as far-field patterns, radiation efficiency, and gain must also be carefully examined over the entire frequency band.



Figure 8. Photograph of the fabricated prototypes (left: top view, right: bottom view).

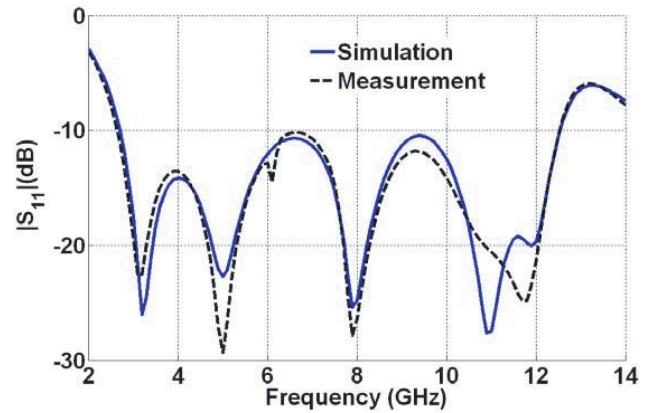


Figure 9. Numerical and experimental reflection coefficient curves of the proposed antenna versus frequency.

The co- and cross-polar far-field radiation patterns of the antenna were measured at different frequencies. For brevity, the numerical and experimental H (x - z)- and E (y - z)-plane patterns at only 3, 7, and 12 GHz are compared in Figure 10. In this figure, E_θ -field and E_φ -field are co- and cross-polar components, respectively. A reasonable concordance between the numerical and experimental outcomes is seen. It is observed that the antenna provides nearly omnidirectional and bidirectional patterns in the H - and E -plane, respectively. As shown in this figure, the magnitude of cross-polarized component is acceptable at lower frequencies, while it increases at higher frequencies. The increase in cross-polarization level is due to the excitation of hybrid currents at high frequencies.

Figure 11 illustrates the experimental and numerical gains and radiation efficiencies of the proposed antenna versus frequency. As shown in Figure 11(a), the maximum value of the measured antenna gain is 4.5 dBi which occurs at 11 GHz. It should be pointed out that the measured gain of the antenna is moderate at the desired frequency range respecting the compact size and omnidirectional behavior of the antenna. Besides, as shown in Figure 11(b), the fabricated antenna can provide desirable radiation efficiency of greater than 81% over the frequency range of 3–12 GHz. The antenna radiation efficiency is also desirable considering the FR4 substrate with loss tangent of 0.02.

To analyze the time-domain characteristic of the antenna, group delay and fidelity factor parameters are investigated. These time-domain characteristics determine the signal distortion which an antenna adds to its input signal. Notice that the signal distortion reduces signal-to-noise ratio and increases bit error rate in communication systems. In a wideband communication system, the group delay is one of the important characteristics. This parameter can cause pulse distortion, and consequently signal to noise or bit error degradation. In order to provide desirable time-domain behavior, constant group delay is required over the entire working band. Figure 12 presents the experimental and numerical group delay curves of the antenna for face-to-face configuration. To investigate the group delay, the distance between the receiving and transmitting antennas was selected as 40 cm. As shown in Figure 12, the total variation of the measured group delay is limited to less than 1.5 ns over the whole working band. The results indicate that the fabricated SCPBTA has an acceptable time domain characteristic. Although not shown, similar results for side-by-side case were obtained.

The fidelity factor is generally preferred as a time domain performance parameter. In the last step of this work, fidelity factor is calculated by using CST Microwave Studio. By utilizing the approach presented in [28], the input pulse is delivered to the antenna, and the E_θ component of electric field in the far-field region is received via seven virtual probes. The distance between the transmitting antenna and the probes maintains at 40 cm. The fidelity factor is calculated in both E - and H -planes. In each plane, seven probes are located with the angle equal to 0° , 15° , 30° , 45° , 60° , 75° , and 90° , respectively. The calculated fidelity factor for both planes is plotted in Figure 13. As it can be observed, the fidelity factor in both planes is more than 0.82, making the antenna suitable for most practical UWB applications.

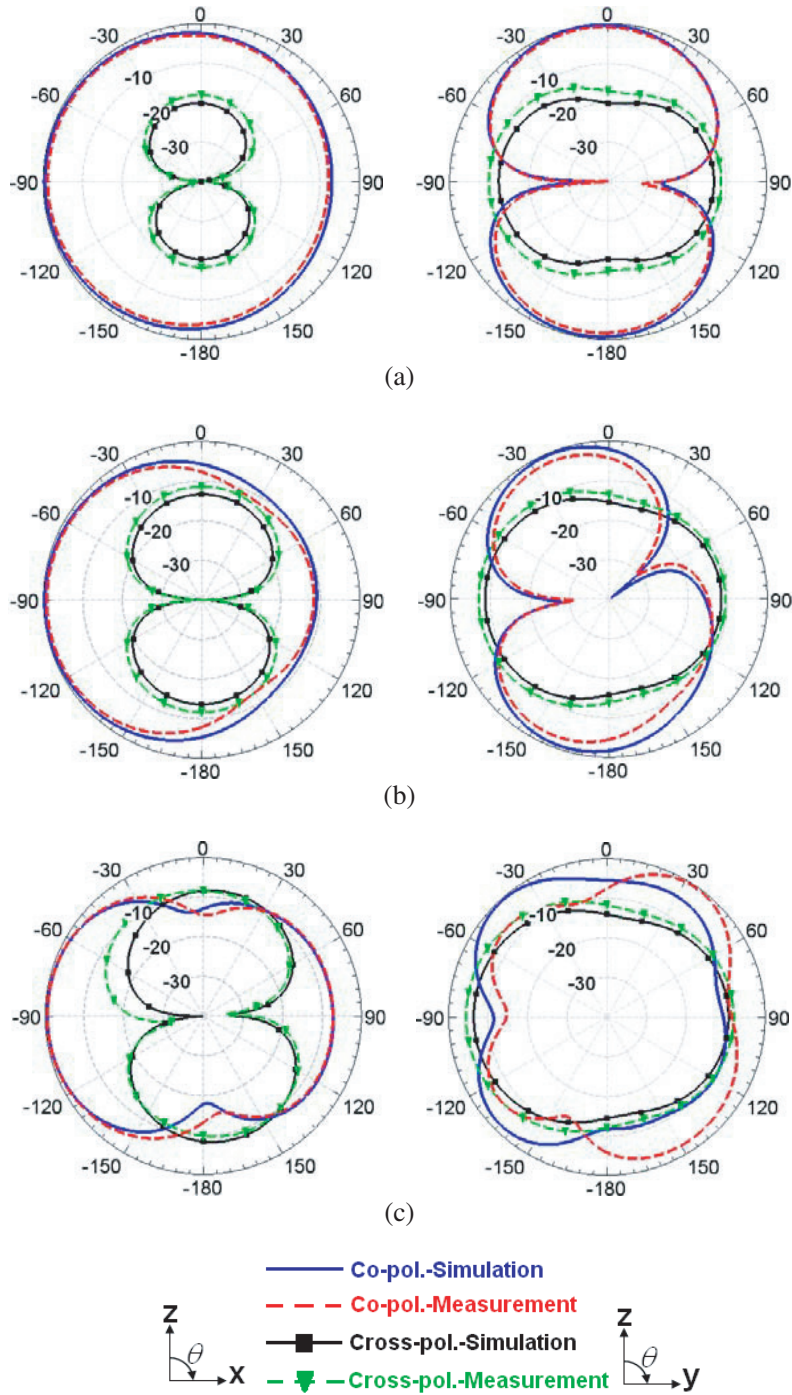


Figure 10. Experimental and numerical co- and cross-polar far-field patterns of the antenna (left: *H*-plane, right: *E*-plane). (a) At 3 GHz. (b) At 7 GHz. (c) At 12 GHz.

It is worth mentioning that the proposed antenna has an overall size of $28 \times 28 \text{ mm}^2$, which is less than the size of the presented antennas in [25] and [26] with dimensions of $50 \times 50 \text{ mm}^2$ and $48 \times 42 \text{ mm}^2$, respectively. The impedance bandwidths of the antennas in [25] and [26] are 118.8% (2.8–11 GHz) and 125% (3–13 GHz), respectively, whereas the impedance bandwidth of the antenna in this design is 129% (2.7–12.55 GHz). This comparison verifies the advantages of the design procedure.

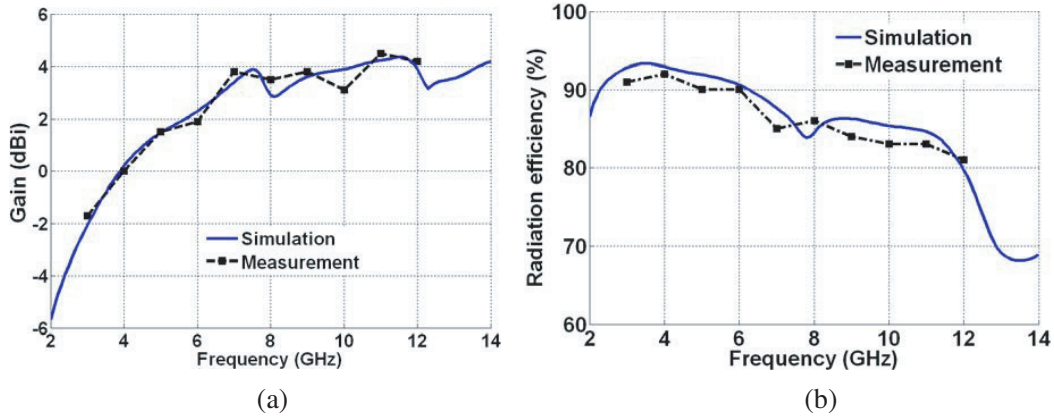


Figure 11. Numerical and experimental radiation parameters of the antenna versus frequency. (a) Gain. (b) Radiation efficiency.

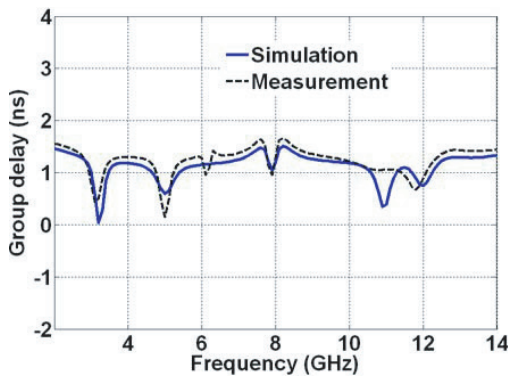


Figure 12. Experimental and numerical group delay curves of the antenna versus frequency.

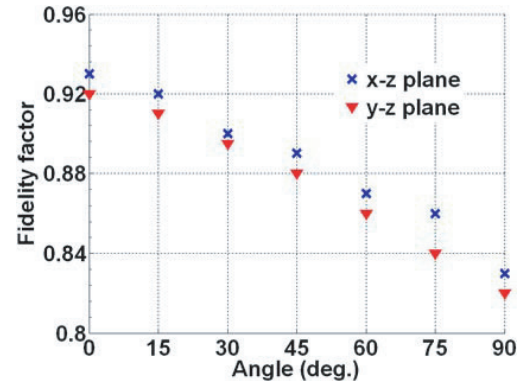


Figure 13. Calculated fidelity factor of the antenna.

4. CONCLUSION

This paper presents a compact planar UWB antenna with simple structure. In order to jointly achieve UWB performance with a compact size, two open ended rounded inverted L-shaped slots are etched on the square ground plane. Further bandwidth enhancement is obtained by cutting a bevel on the asymmetrical radiating patch. Moreover, to improve the impedance matching of the antenna at the middle frequencies, a small inverted L-shaped slot is etched on the ground plane. The experimental and numerical results of the proposed antenna in both time- and frequency-domain have been presented and discussed. Measured results show that the proposed antenna with a small size of $28 \times 28 \times 1.6 \text{ mm}^3$ has a wide impedance bandwidth of more than 129% from 2.7 to 12.55 GHz (for $|S_{11}| < -10 \text{ dB}$). The evolution procedure of the proposed antenna is presented and several designs are investigated. It is shown that by introducing several antenna designs, the impedance bandwidth can be enhanced from 58% to 129%. A numerical sensitivity analysis has been carried out to understand the effects of the key design parameters on the antenna impedance bandwidth. Experimental results for the reflection coefficient, far-field radiation patterns, radiation efficiency, gain, and group delay of the designed antenna are presented and compared with the simulation data. Also, the fidelity factor is calculated in both E - and H -planes by using CST Microwave Studio. Compared with the recent designs presented in [25] and [26], the designed antenna has a smaller size and wider bandwidth. The measured outcomes show that the antenna is a competent option for the use in UWB communication systems.

REFERENCES

1. Li, G., H. Zhai, T. Li, X. Ma, and C.-H. Liang, "Design of a compact UWB antenna integrated with GSM/WCDMA/WLAN bands," *Progress In Electromagnetics Research*, Vol. 136, 409–419, 2013.
2. Lizzi, L., G. Oliveri, and A. Massa, "A time-domain approach to the synthesis of UWB antenna," *Progress In Electromagnetics Research*, Vol. 122, 557–575, 2012.
3. Zhang, Z. and Y. H. Lee, "A robust CAD tool for integrated design of UWB antenna systems," *Progress In Electromagnetics Research*, Vol. 112, 441–457, 2011.
4. Habib, M. A., A. Bostani, A. Djaiz, M. Nedil, M. C. E. Yagoub, and T. A. Denidni, "Ultra wideband CPW-fed aperture antenna with WLAN band rejection," *Progress In Electromagnetics Research*, Vol. 106, 17–31, 2010.
5. Yu, C.-C. and X.-C. Lin, "A wideband single chip inductor-loaded CPW-fed inductive slot antenna," *IEEE Transactions on Antennas and Propagation*, Vol. 56, No. 5, 1498–1501, May 2008.
6. Li, X. L., Y.-Z. Yin, P. A. Liu, J. H. Wang, and B. Xu, "A CPW-fed dual band-notched UWB antenna with a pair of bended dual-L-shape parasitic branches," *Progress In Electromagnetics Research*, Vol. 136, 623–634, 2013.
7. Chen, D. and C.-H. Cheng, "A novel compact ultra-wideband (UWB) wide slot antenna with via holes," *Progress In Electromagnetics Research*, Vol. 94, 343–349, 2009.
8. Jiao, J.-J., G. Zhao, F.-S. Zhang, H.-W. Yuan, and Y.-C. Jiao, "A broadband CPW-fed T-shape slot antenna," *Progress In Electromagnetics Research*, Vol. 76, 237–242, 2007.
9. Liang, X. L., T. A. Denidni, L. N. Zhang, R. H. Jin, J. P. Geng, and Q. Yu, "Printed binomial-curved slot antennas for various wideband applications," *IEEE Transactions on Microwave Theory and Techniques*, Vol. 59, No. 4, 1058–1065, Apr. 2011.
10. Sze, J.-Y., C.-I. G. Hsu, and S.-C. Hsu, "Design of a compact dual-band annular-ring slot antenna," *IEEE Antennas and Wireless Propagation Letters*, Vol. 6, 423–426, 2007.
11. Krishna, D. D., M. Gopikrishna, C. K. Anandan, P. Mohanan, and K. Vasudevan, "CPW-fed koch fractal slot antenna for WLAN/WiMAX applications," *IEEE Antennas and Wireless Propagation Letters*, Vol. 7, 389–392, 2008.
12. Jan, J. Y. and L. C. Wang, "A study on broadband printed slot antennas with regular rhombus slots," *Proc. IEEE Region 10 Conference (TENCON)*, 1–3, Taipei, Taiwan, Oct. 30–Nov. 2, 2007.
13. Li, P., J. Liang, and X. Chen, "Study of printed elliptical/circular slot antennas for ultrawideband applications," *IEEE Transactions on Antennas and Propagation*, Vol. 54, No. 6, 1670–1675, Jun. 2006.
14. Chen, W. S., "A novel broadband design of a printed rectangular slot antenna for wireless communications," *Microwave Journal*, Vol. 49, No. 1, 122–130, Jul. 2006.
15. Chen, W. S. and F. M. Hsieh, "A broadband design for a printed isosceles triangular slot antenna for wireless communications," *Microwave Journal*, Vol. 48, No. 7, 98–112, Jul. 2005.
16. Chiou, J.-Y., J.-Y. Sze, and K.-L. Wong, "A broad-band CPW-fed strip-loaded square slot antenna," *IEEE Transactions on Antennas and Propagation*, Vol. 51, No. 4, 719–721, Apr. 2003.
17. Chen, H.-D., "Broadband CPW-fed square slot antennas with a widened tuning stub," *IEEE Transactions on Antennas and Propagation*, Vol. 51, No. 4, 1982–1986, Aug. 2003.
18. Chair, R., A. A. Kishk, and K. F. Lee, "Ultrawideband coplanar waveguide-fed rectangular slot antenna," *IEEE Antennas and Wireless Propagation Letters*, Vol. 3, 227–229, 2004.
19. Lee, H. L., H. J. Lee, J. G. Yook, and H. K. Park, "Broadband planar antenna having round corner rectangular wide slot," *Proc. IEEE Antennas and Propagation Society Int. Symp.*, Vol. 2, 460–463, Jun. 16–21, 2002.
20. Eskandari, H., M. R. Booket, M. Kamyab, and M. Veysi, "Investigation on a class of wideband printed slot antenna," *IEEE Antennas and Wireless Propagation Letters*, Vol. 9, 1221–1224, 2010.
21. Liu, Y. F., K. L. Lau, Q. Xue, and C. H. Chan, "Experimental studies of printed wide-slot antenna for wide-band applications," *IEEE Antennas and Wireless Propagation Letters*, Vol. 3, 273–275,

- 2004.
22. Sung, Y., "Bandwidth enhancement of a microstrip line-fed printed wide-slot antenna with a parasitic center patch," *IEEE Transactions on Antennas and Propagation*, Vol. 60, No. 4, 1712–1716, Apr. 2012.
 23. Liu, W. X., Y. Z. Yin, W. L. Xu, and S. L. Zuo, "Compact open-slot antenna with bandwidth enhancement," *IEEE Antennas and Wireless Propagation Letters*, Vol. 10, 850–1224, 2011.
 24. Xu, K., Z. Zhu, H. Li, J. Huangfu, C. Li, and L. Ran, "A printed single-layer UWB monopole antenna with extended ground plane stubs," *IEEE Antennas and Wireless Propagation Letters*, Vol. 12, 237–240, 2013.
 25. Siddiqui, J. Y., C. Saha, and Y. M. M. Antar, "A novel ultrawideband (UWB) printed antenna with a dual complementary characteristic," *IEEE Antennas and Wireless Propagation Letters*, Vol. 14, 974–977, 2015.
 26. Unnikrishnan, D., D. Kaddour, S. Tedjini, E. Bihar, and M. Saadaoui, "CPW-fed inkjet printed UWB antenna on ABS-PC for integration in molded interconnect devices technology," *IEEE Antennas and Wireless Propagation Letters*, Vol. 14, 1124–1128, 2015.
 27. Dastranj, A. and B. Abbasi-Arand, "Investigation of a low-profile planar monolayer UWB antenna with an open slot for bandwidth enhancement," *Progress In Electromagnetics Research C*, Vol. 59, 175–185, 2015.
 28. Wu, Q., R. Jin, J. Geng, and M. Ding, "Pulse preserving capabilities of printed circular disk monopole antennas with different grounds for the specified input signal forms," *IEEE Transactions on Antennas and Propagation*, Vol. 55, No. 10, 2866–2873, Oct. 2007.